REVISTA MATÉRIA V.29 N.2
ISSN 1517-7076 articles e20240010, 2024

Numerical simulation of confinement effect of CFRP and GFRP strengthened concrete specimens

Vijayakumar Arumugam[1], Senguttuvan Kavipriya[2], Mohammed Nabi Anwar Gulshan Taj[3], Muthaiyan Periyasamy[4]

[1]V.S.B. Engineering College, Department of Civil Engineering. 639111, Karur, Tamil Nadu, India.

[2]Kongunadu College of Engineering and Technology, Department of Civil Engineering. 621215, Trichy, Tamil Nadu, India.

[3]Sona College of Technology, Department of Civil Engineering. 636005, Salem, Tamil Nadu, India.

[4]Rajalakshmi Engineering College, Department of Civil Engineering. 602105, Chennai, Tamil Nadu, India.

e-mail: vijayakumarkct@gmail.com, kavipriyas@gmail.com, drgulshaniit@gmail.com, muthaiyanpcivil@gmail.com

ABSTRACT

For structural strengthening and retrofitting, advanced composite materials like carbon fiber reinforced polymer (CFRP) and glass fiber reinforced polymer (GFRP) are frequently utilized. Applications in civil engineering require a thorough understanding of the behaviour and response of such materials. To forecast the stress-strain behaviour, the current research focuses on the numerical simulation of CFRP and GFRP-reinforced concrete specimens. ABAQUS was used to model a concrete specimen using the C3D8R solid element. The material modeling has considered the nonlinear compression behaviour of concrete and the linear elastic compression behaviour of CFRP/GFRP. The research examined gains in load-carrying capacity compared to concrete of normal strength and confined to unconfined strengths. The validity of numerical simulation has been confirmed through comparison with published experimental results. Additionally, the impact of the number of layers is carefully examined. Additionally, a comparison of the stress-strain characteristics of specimens enhanced with GFRP and CFRP has been conducted.

Keywords: CFRP; GFRP; Reinforced concrete; FRP Laminates; Three-point bending test.

1. INTRODUCTION

Recent earthquakes have brought to light several existing reinforced concrete structures' problematic behaviours and the requirement for suitable retrofit solutions. Most current seismic retrofit solutions concentrate on improving a structure's mechanical qualities, such as its strength and stiffness. The usage of composite materials for the rehabilitation of seismically weak RC structures has increased during the past several years on a global scale. The RC columns need to be laterally constrained for substantial deformation under load and acceptable resistance capability. Energy dissipation permitted by a tightly confined concrete core during a seismic event frequently prevents the loss of human life. Conversely, a concrete column with inadequate constraint displays brittle behavior that may result in unanticipated, disastrous failures. Once the steel has yielded, steel jacketing provided by hoops or ties applies a steady restricting pressure. When a fully elastic material, such as FRP, is used, volumetric expansion increases and the restrictive force on concrete increases with the load. Understanding this novel behaviour is necessary, and the theory must be approached differently.

The corrosive nature of steel causes concrete Steel's decreased strength and ductility cause constructions made with it to degrade over time. Because of its remarkable ability to withstand corrosion, low density, high strength, low thermal conductivity, and electromagnetic susceptibility, GFRP material has emerged as the most potential substitute [1–4]. These anisotropic composite materials prolong the service life of reinforced concrete in abrasive and hostile conditions and help save operating costs [2, 5]. Advanced study focuses on how plain concrete becomes less fragile. Polyvinyl alcohol (PVA) and polypropylene fiber (PF) fibers were added to the concrete to improve its ductility and decrease its brittleness. Also, other research showed that concrete columns reinforced with steel fibers and bars had greater ductility and strength [6, 7].

An analytical buckling model based on numerical integration has presented to predict the load versus deflection performance of slender concrete columns reinforced with fibre-reinforced polymer (FRP) spirals and longitudinal bars, subjected to eccentric loads. The model can be used to predict the behavior of slender

Corresponding Author: Vijayakumar Arumugam Received on 11/01/2024 Accepted on 05/03/2024

DOI: https://doi.org/10.1590/1517-7076-RMAT-2024-0010

concrete columns with various configurations including FRP and/or steel reinforcement, single or double spiral, and number of longitudinal bars. The longitudinal bars considered include steel, FRP, or hybrid reinforcement consisting of steel and FRP bars. The model was found to predict the experimental performance of slender concrete columns reinforced with Glass FRP longitudinal bars and spirals with satisfactory accuracy. The model is used to create interaction diagrams for FRP spiral-confined circular concrete columns with various slenderness ratios, reinforced with steel, FRP or hybrid reinforcement [8].

Rather than rupture, the bond-slip process usually leads to the failure of GFRP lateral reinforcement [9]. Because of their linear elastic behavior, GFRP-RC columns have not yet displayed any balance points [10]. Except for GFRP-RC columns' 7% lower axial strength (AS), the behavior of the steel and GFRP-RC compression members was comparable [11]. In the laterally confined GFRP-RC columns with a 76 mm pitch, the axial strength (AS) of 84% of their steel-RC column counterparts was noted [12]. GFRP bars work better in concrete when squeezed because they have a lower elastic modulus than steel bars; this makes utilizing GFRP bars in concrete columns desirable. [13]. Using the steel reinforcement with a comparable number of GFRP bars improved column ductility under various loading situations while lowering the axial and bending strengths [14]. Reducing the stirrups' vertical spacing has significantly increased the ductility of GFRP-RC columns [15–17].

The present investigation [18] aims to propose a numerical model for assessing the complex damaging response of glass fiber reinforced polymer- (GFRP-) reinforced concrete columns having hybrid fibers and confined with GFRP spirals (Glass Fiber Hybrid Fibers - GFHF columns) under concentric and eccentric compression. Fiber-reinforced concrete (FRC) consists of polyvinyl alcohol fibers (PVA) and polypropylene fibers (PF). A commercial package ABAQUS was used for the finite element analysis (FEA) The results depicted that the failure of GFHF columns occurred either in the upper or in the lower half portion with the rupture of GFRP longitudinal bars and GFRP spirals. The decrease in the pitch of GFRP spirals led to an improvement in the axial strength (AS) of GFHF columns. The eccentric loading caused a significant reduction in the AS of columns. The comparative study solidly substantiates the validity and applicability of the newly developed FEA models for capturing the AS of GFHF columns by considering the axial involvement of longitudinal GFRP bars and the confinement effect of transverse GFRP spirals. So, the suggested numerical model having a complex system of equations for HFRC can be used for the accurate analysis of HFRC members. This work aims to simulate the stress-strain behaviour of CFRP numerically, and GFRP strengthened concrete cylinder to assess the confinement effect. For this, ABAQUS is used to model the linear and nonlinear behaviour of CFRP/GFRP and concrete, respectively. Studying the improvement in confinement also takes into account the number of layers.

1.1. Finite element modelling issues

Accurate stress/deformation estimation necessitates intricate component modelling for a structure with wrapping. The FE model used in the investigations significantly impacts how accurate the response is. The analysis can make use of numerous FE models and formulations. Three-dimensional elements, the thin/thick shell formulation (Reissner-Mindlin theory), the thin-shell formulation (Kirchoff theory), and facet plate/shell elements can all be used to represent them. Model plate/shell panels are typically favored over shell parts.

2. MATERIAL NONLINEARITY

When a significant force is applied to the structure or component, the resulting stresses could be greater than the yield strength of the material. The material's multilinear stress-strain relationship can be used in this case to take plastic deformation into account. Important ideas for simulating inelastic behavior are: Strain breaks down into elastic and plastic components. Two forms of strain are produced by a given stress under uniaxial loading: a small, reversible elastic strain and a large, irreversible plastic strain (Figure 1).

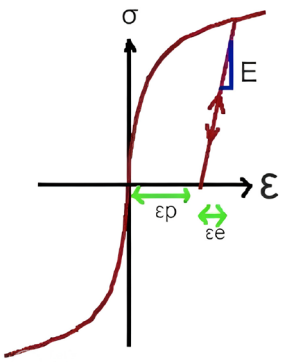

$$\varepsilon = \varepsilon^{e} + \varepsilon^{p} \quad (1)$$

Where

ε = Total Strain

ε^{e} = Elastic Strain

ε^{p} = Plastic Strain

Figure 1: Stress-strain plot under uniaxial tension.

Yield criterion to predict whether the solid response elastically or plastically. Two assumptions underlie the yield criterion: (a) that the solid is isotropic; and (b) that the yield is independent of hydrostatic pressure. Assumption (a) states that the yield requirement can only depend on the deviatoric stress components.

$$S_{ij} = \sigma_{ij} - (\sigma_{kk} / 3)\, \delta_{ij} \tag{2}$$

According to assumption in the equation (2) (b), the direction of the primary stresses cannot affect the commencement of yield; instead, it can only affect their magnitudes, which are σ1, σ2, and σ3. Figure 2 resembles the Visualization of Yield Criteria.

The plastic's stress-strain curve's form is governed by strain hardening laws. The easiest way to model strain hardening is to make the yield surface increase in size, but remain the same shape, as a result of plastic straining. Below, in Figure 3, are examples of some of the more typical hardening stress-strain functions.

The plastic stresses caused by loading above yield must be calculated to finish the constitutive model. Applying a stress σ_{ij} that is exactly right to obtain yield will do this. The tension should now be increased to $\sigma_{ij} + d\sigma_{ij}$. Next, calculate the plastic strain increment $d\varepsilon_{ij}$ that results. The solid's behaviour during hardening determines the plastic strain's size. This is so that the stress during continuous plastic flow is always on the yield surface. The plastic strain magnitude must be linked to the stress increment because the yield surface's radius (or the location for kinematic hardening) is correlated with the amount of the plastic strain increase by an appropriate hardening equation.

2.1. The criteria of elastic unloading represent the irreversible behavior

It is generally understood that plastic movement is irreversible and constantly loses energy. There won't be any plastic strain if the stress increase d_{ij} is tangent to the yield surface or lowers the stress to yield. Elastic unloading is depicted in Figure 4.

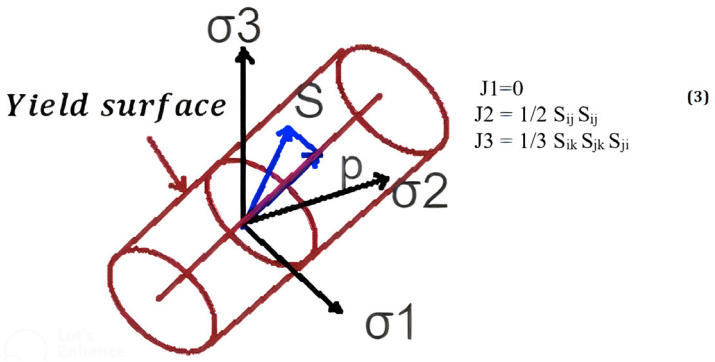

Figure 2: Visualization of yield criteria.

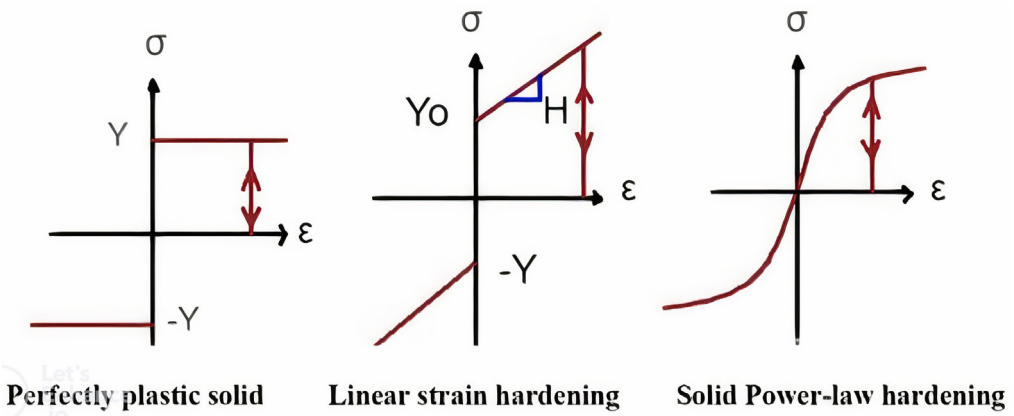

Figure 3: Common forms of hardening functions.

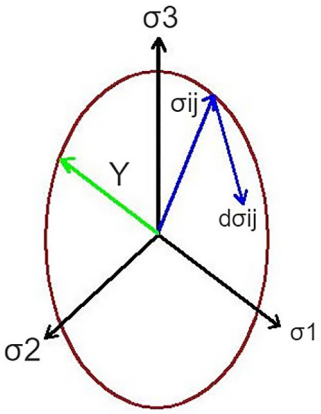

Figure 4: Elastic unloading condition.

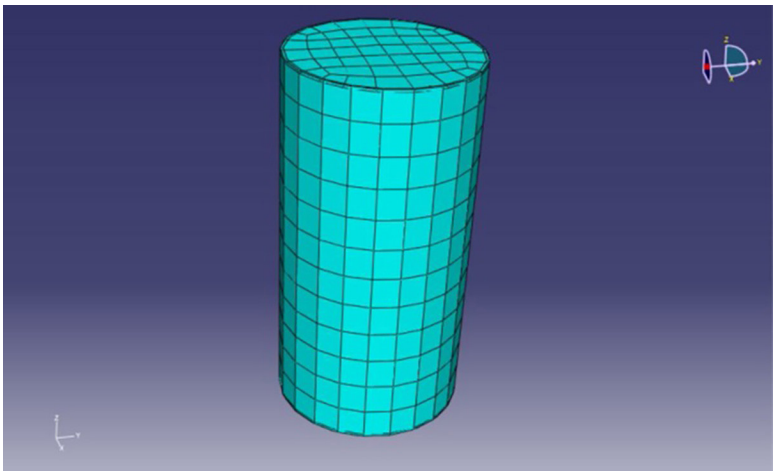

Figure 5: Typical FE model.

Strengthening using CFRP/GFRP requires analytical tools that predict the level of confinement effect which enhances the performances of concrete core. Numerous research has been carried out as part of this endeavor to assess the confinement effectiveness of CFRP/GFRP strengthening. An analytical method utilising finite elements has been used to analyse the ductility of cylindrical specimens of normal strength concrete that are both confined and unconfined. The cylinder is 150 mm by 300 mm. Modeling is done using the C3D8R solid element on concrete and CFRP/GFRP specimens. In Figure 5, the usual FE model is displayed.

3. MATERIAL MODELLING

The grade of concrete used for modelling is M25. A Piecewise plasticity model for concrete is adopted to account for nonlinearity (Figure 6).

For the case of GFRP/CFRP, only linear elastic properties are considered. The modulus of elasticity for GFRP is 18333 MPa and 120000 MPa [19] for CFRP. Poisson's ratio for both materials is 0.15 [19]. Regarding boundary conditions, bottom surface of the cylinder is considered as fixed. The cylinder's top surface can only move in an axial direction [20–22] (Figure 7). A displacement-controlled approach carries out analysis.

4. INTERFACE MODELLING

4.1. Surface-to-surface contact

The interface between the concrete specimen encased by CFRP has been modelled using ABAQUS' surface-to-surface contact algorithm. The true surface-to-surface method optimizes the stress accuracy for a

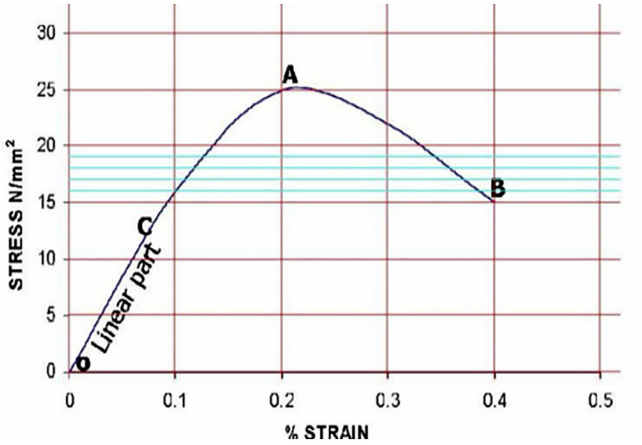

Figure 6: Stress-strain plot for concrete.

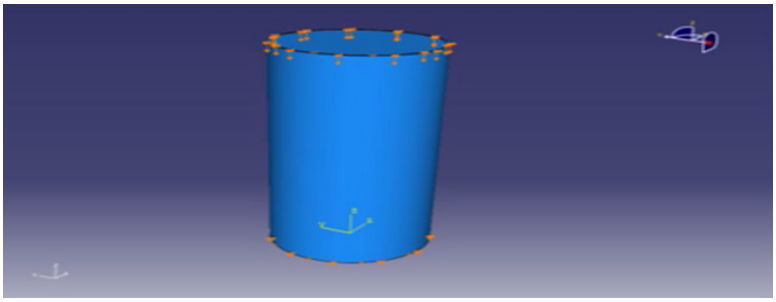

Figure 7: Model with boundary conditions.

certain surface pairing [23–26]. The correctness of the solution can be significantly impacted by choice of slave and master surfaces. In this investigation, CFRP was used as the master surface, while concrete was used as the slave surface. In mechanical contact simulations, a finite sliding tracking technique is utilized to consider the relative motion of the two surfaces constituting a contact pair. Finite sliding methods have been applied in the current investigation. In a finite-sliding contact, the relative tangential motion of the contacting surfaces causes a change in the connectedness of the contact constraints that are currently in effect. The only way that can be utilised to enforce connections with softened pressure over closure is the direct method. The direct approach has been considered for constraint enforcement. For surface-based contact, a hard contact pressure-overclosure relationship is employed [27–35].

4.2. Cohesive model

To replicate the behaviour of the interface between concrete and CFRP, a cohesive model has been created. The cohesive model's characteristics are primarily for bonded interfaces with extremely thin interfaces, which can be used to describe the glue between concrete and FRP [36, 37]. In these circumstances, it might be simple to define the cohesive layer's constitutive response in terms of traction versus separation. Therefore, traction separation is a direct definition of cohesive behaviour. Therefore, traction separation is a direct definition of cohesive behaviour [38]. In cases where the cohesive layer's discretization level differs from the surrounding structures', which are usually finer in discretization, the cohesive layer's top and/or bottom surfaces can be tied to the surrounding structures using a tie constraint if the two neighboring parts do not have matched meshes. Two dissimilar components are joined together by cohesive aspects. As a result of the deformation, the cohesive parts frequently deteriorate under tension and/or shear [39–42]. Cohesive factors that are originally holding the components together may later meet one another. Modulus of elasticity of epoxy has been taken as 1066 MPa, Poisson's ratio 0.43 and modulus of rigidity 745 has been used as input. An 8-node three dimensional cohesive element (COH3D8) has been accounted for material modelling in the present study.

4.3. Analysis

There are two approaches for analysis: load controlled, and displacement controlled. In the load-controlled approach, load is applied, displacement is calculated for corresponding loading, and displacement-controlled load is calculated for corresponding displacements. Here, analysis is carried out by a displacement-controlled approach because the displacement-controlled analysis can accurately capture post-peak response behaviour.

5. RESULT AND DISCUSSION

Static nonlinear analysis has been carried out for plain and CFRP confined concrete specimens. Figure 8 shows that the computed and related experimental/analytical results are in good accordance. The stress-strain behaviour obtained is shown in Figure 8.

Surface-to-surface and cohesive model stress-strain behaviour are shown in Figure 9. As seen in Figure 9, the cohesive model is flexible in the nonlinear range while stiffer in the linear range compared to the surface-to-surface and surface model [43].

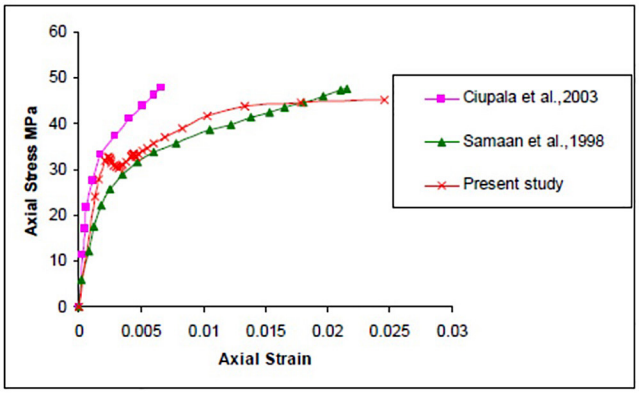

Figure 8: Axial stress-strain plot for CFRP.

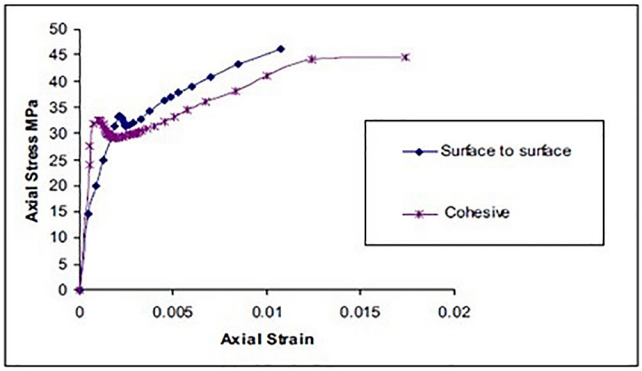

Figure 9: Axial stress-strain plot for surface to surface & cohesive model.

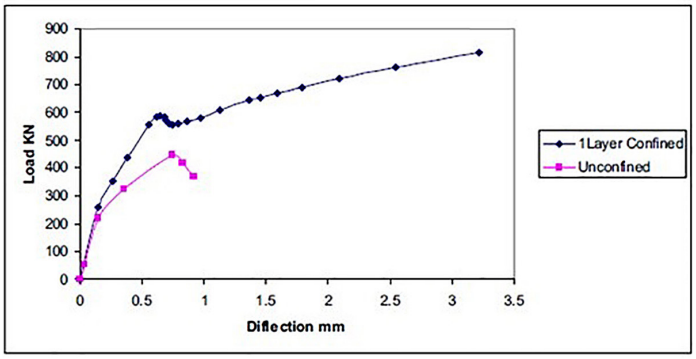

Figure 10: Load vs deflection.

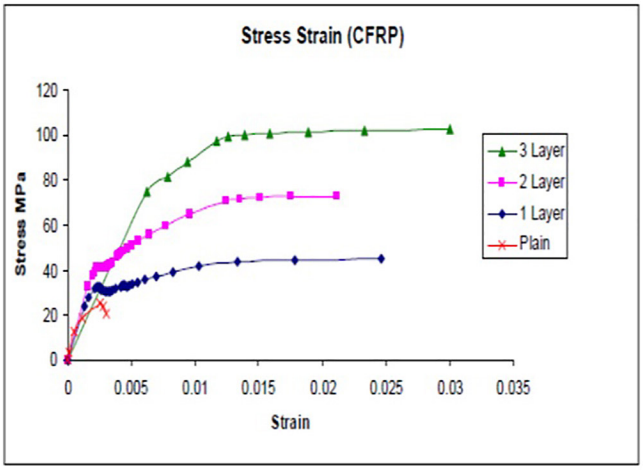

Figure 11: Axial stress-strain plot for CFRP.

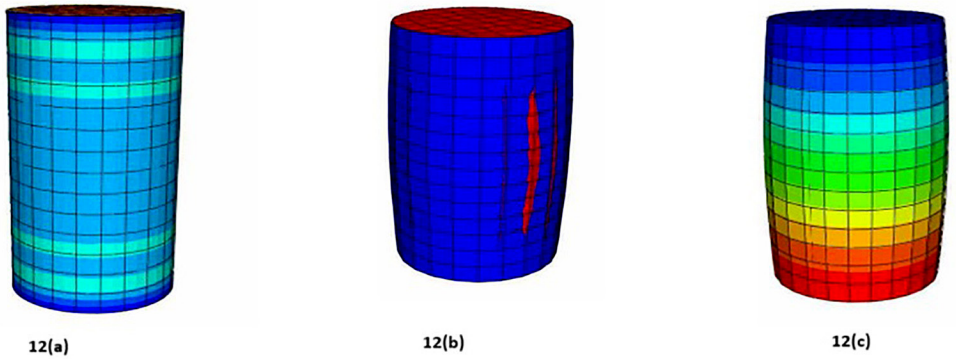

Figure 12: (a) Axial stress; (b) traction separation; (c) displacement contour.

Figure 10 illustrates the increase in load-carrying capability brought on by the confinement of CFRP. The ultimate load has increased by nearly 80%. Additionally, it should be observed that the specimen's ductility grows stronger with confinement [44].

5.1. Sensitivity analysis

For CFRP, a sensitivity analysis has been done in relation to the number of wrapping layers. A cylinder with different wrapping layers (1, 2, and 3) has undergone a finite element analysis while maintaining a constant compressive strength of concrete [45]. The axial stress-strain behaviour of CFRP with 1, 2, and 3 layers is plotted in Figure 11. Axial stress rises as the number of layers increases, as shown in Figure 11. Comparing 3-layered confinement to 1 and 2-layered confinement, the stiffness reduces. Third layerd confinement experienced reduction in stiffness compared with 1- and 2-layer confinement after elastic state.

The axial stress contour obtained from the analysis and the traction separation with CFRP with concrete and the displacement contour are shown in Figure 12(a–c).

6. CONCLUSION

Numerical simulation of CFRP strengthened concrete specimens to predict the stress-strain behavior has been carried out. The concrete specimen has been modelled by using ABAQUS employing solid element. The material modelling has considered concrete's nonlinear compression behaviour and CFRP's linear elastic compression behaviour. An interface model has been developed using cohesive model option available in ABAQUS. The response behaviour using cohesive model has been compared with surface to surface contact option between concrete and CFRP. The study has been conducted in terms of gains in load carrying capacity compared to the concrete specimen that had not been strengthened and confined to unconfined strengths. The performance of

interface modelling using cohesive and surface-to-surface models has been compared. It is found that the surface-to-surface model stiffer in the non-linear region compared to the cohesive model. The effect of the number of layers has also been studied in detail for 1, 2, and 3 layers of CFRP wrapping. It is observed that axial stress increases with the number of layers in the case of CFRP confinement up to two layers. For three confinement layers, the stress-strain behavior is observed to be flexible. This may be due to the debonding between the layers of CFRP. From the overall study it is concluded that the load carrying capacity increases by using confinement. There is an optimum value of the number of layer of CFRP layers for which axial stress increases with the increase in strain. The CFRP wrapping is a helpful option for retrofitting applications.

7. BIBLIOGRAPHY

[1] ZADEH, H.J., NANNI, A., "Design of RC columns using glass FRP reinforcement", *Journal of Composites for Construction*, v. 17, n. 3, pp. 294–304, 2012. doi: http://dx.doi.org/10.1061/(ASCE)CC.1943-5614.0000354.

[2] RAZA, A., KHAN, Q.U.Z., AHMAD, A., "Numerical investigation of load-carrying capacity of GFRP-reinforced rectangular concrete members using CDP model in ABAQUS", *Advances in Civil Engineering*, v. 2019, pp. 1745341, 2019. doi: http://dx.doi.org/10.1155/2019/1745341.

[3] ELCHALAKANI, M., DONG, M., KARRECH, A., *et al*., "Circular concrete columns and beams reinforced with GFRP bars and spirals under axial, eccentric, and flexural loading", *Journal of Composites for Construction*, v. 24, n. 3, pp. 04020008, 2020. doi: http://dx.doi.org/10.1061/(ASCE)CC.1943-5614.0001008.

[4] RAZA, A., RAHEEL SHAH, S.A., KHAN, M.M., *et al*., "Axial load-carrying capacity of steel tubed concrete short columns confined with advanced FRP composites", *Periodica Polytechnica. Civil Engineering*, v. 64, n. 3, 2020. doi: http://dx.doi.org/10.3311/PPci.15199.

[5] BENMOKRANE, B., EL-SALAKAWY, E., EL-RAGABY, A., *et al*., "Designing and testing of concrete bridge decks reinforced with glass FRP bars", *Journal of Bridge Engineering*, v. 11, n. 2, pp. 217–229, 2006. doi: http://dx.doi.org/10.1061/(ASCE)1084-0702(2006)11:2(217).

[6] RAZA, A., KHAN, Q.U.Z., "Experimental and numerical behavior of hybrid fiber reinforced concrete compression members under concentric loading," *SN Applied Sciences*, vol. 2, pp. 701, 2020. doi: http://dx.doi.org/10.1007/s42452-020-2461-5.

[7] PAULTRE, P., EID, R., LANGLOIS, Y., *et al*., "Behavior of steel fiber-reinforced high-strength concrete columns under uniaxial compression", *Journal of Structural Engineering*, v. 136, n. 10, pp. 1225–1235, 2010. doi: http://dx.doi.org/10.1061/(ASCE)ST.1943-541X.0000211.

[8] HALES, T.A., PANTELIDES, C.P., REAVELEY, L.D., "Analytical buckling model for slender FRP-reinforced concrete columns", *Composite Structures*, v. 176, pp. 33–42, 2017. doi: http://dx.doi.org/10.1016/j.compstruct.2017.05.034.

[9] DONG, H.-L., WANG, Z., SUN, Y., "Axial compressive behavior of square concrete columns reinforced with innovative closed-type winding GFRP stirrups", *Composite Structures*, v. 192, pp. 115–125, 2018. doi: http://dx.doi.org/10.1016/j.compstruct.2018.02.092.

[10] WANG, C.C., HARIK, I.E., GESUND, H., "Strength of rectangular concrete columns reinforced with fiber-reinforced polymer bars", *ACI Structural Journal*, v. 103, n. 3, pp. 452, 2006.

[11] AFIFI, M.Z., MOHAMED, H.M., BENMOKRANE, B., "Axial capacity of circular concrete columns reinforced with GFRP bars and spirals", *Journal of Composites for Construction*, v. 18, n. 1, pp. 04013017, 2013. doi: http://dx.doi.org/10.1061/(ASCE)CC.1943-5614.0000438.

[12] PANTELIDES, C.P., GIBBONS, M.E., REAVELEY, L.D., "Axial load behavior of concrete columns confined with GFRP spirals", *Journal of Composites for Construction*, v. 17, n. 3, pp. 305–313, 2013. doi: http://dx.doi.org/10.1061/(ASCE)CC.1943-5614.0000357.

[13] SUN, L., WEI, M., ZHANG, N., "Experimental study on the behavior of GFRP reinforced concrete columns under eccentric axial load", *Construction & Building Materials*, v. 152, pp. 214–225, 2017. doi: http://dx.doi.org/10.1016/j.conbuildmat.2017.06.159.

[14] HADI, M., KARIM, H., SHEIKH, M.N., "Experimental investigations on circular concrete columns reinforced with GFRP bars and helices under different loading conditions", *Journal of Composites for Construction*, v. 20, n. 4, pp. 04016009, 2016. doi: http://dx.doi.org/10.1061/(ASCE)CC.1943-5614.0000670.

[15] ELCHALAKANI, M., MA, G., ASLANI, F., *et al*., "Design of GFRP-reinforced rectangular concrete columns under eccentric axial loading", *Magazine of Concrete Research*, v. 69, n. 17, pp. 865–877, 2017. doi: http://dx.doi.org/10.1680/jmacr.16.00437.

[16] KARIM, H., SHEIKH, M.N., HADI, M.N.S., "Axial load-axial deformation behaviour of circular concrete columns reinforced with GFRP bars and helices", *Construction & Building Materials*, v. 112, pp. 1147–1157, 2016. doi: http://dx.doi.org/10.1016/j.conbuildmat.2016.02.219.

[17] MOHAMMED, H.J., ZAIN, M.F.M., "Simulation assessment and theoretical verification of a new design for portable concrete barriers", *KSCE Journal of Civil Engineering*, v. 21, n. 3, pp. 851–862, 2017. doi: http://dx.doi.org/10.1007/s12205-016-0603-5.

[18] ALI, L., NAWAZ, A., BAI, Y., *et al*., "Numerical simulations of GFRP-reinforced columns having polypropylene and polyvinyl alcohol fibers", *Complexity*, v. 2020, pp. 8841795, 2020. doi: http://dx.doi.org/10.1155/2020/8841795.

[19] SONELASTIC – ADVANCED IMPULSE EXCITATION TECHNIQUES. Modulus of elasticity and Poisson's coefficient of polymeric materials. https://www.sonelastic.com/en/fundamentals/tables-of-materials-properties/polymers.html, accessed in March, 2024.

[20] VIJAYAKUMAR, A., VENKATESHBABU, D.L., "Structural behavior of FRP wrapped beams under experimental investigation", *International Journal of Earth Sciences and Engineering*, vol. 5, n. 5, pp. 1377-1383, 2012.

[21] VIJAYAKUMAR, A., VENKATESHBABU, D.L., "Pushover analysis of existing reinforced concrete framed structures", *European Journal of Scientific Research*, v. 71, n. 2, pp. 195–202, 2012.

[22] YANG, L., YE, M., HUANG, Y., *et al*., "Study on mechanical properties of displacement-amplified mild steel bar joint damper", *Civil Engineering (Shiraz)*, 2023. doi: http://dx.doi.org/10.1007/s40996-023-01268-7.

[23] KONG, G., SUN, G., LIU, H., *et al*., "Dynamic response of ballastless track XCC pile-raft foundation under train axle loads", *Journal of Testing and Evaluation*, v. 49, n. 3, pp. 1691–1704, 2021. doi: http://dx.doi.org/10.1520/JTE20180032.

[24] HE, H.E.S., AI, L., WANG, X., *et al*., "Exploiting machine learning for controlled synthesis of carbon dots-based corrosion inhibitors", *Journal of Cleaner Production*, v. 419, pp. 138210, 2023. doi: http://dx.doi.org/10.1016/j.jclepro.2023.138210.

[25] HE, H., SHI, J., YU, S., *et al*., "Exploring green and efficient zero-dimensional carbon-based inhibitors for carbon steel: from performance to mechanism", *Construction & Building Materials*, v. 411, pp. 134334, 2024. doi: http://dx.doi.org/10.1016/j.conbuildmat.2023.134334.

[26] LIU, C., CUI, J., ZHANG, Z., *et al*., "The role of TBM asymmetric tail-grouting on surface settlement in coarse-grained soils of urban area: field tests and FEA modelling", *Tunnelling and Underground Space Technology*, v. 111, pp. 103857, 2021. doi: http://dx.doi.org/10.1016/j.tust.2021.103857.

[27] DENG, E., WANG, Y., ZONG, L., *et al*., "Seismic behavior of a novel liftable connection for modular steel buildings: experimental and numerical studies", *Thin-walled Structures*, v. 197, pp. 111563, 2024. doi: http://dx.doi.org/10.1016/j.tws.2024.111563.

[28] ZHANG, H., XIANG, X., HUANG, B., *et al*., "Static homotopy response analysis of structure with random variables of arbitrary distributions by minimizing stochastic residual error", *Computers & Structures*, v. 288, pp. 107153, 2023. doi: http://dx.doi.org/10.1016/j.compstruc.2023.107153.

[29] WANG, M., YANG, X., WANG, W., "Establishing a 3D aggregates database from X-ray CT scans of bulk concrete", *Construction & Building Materials*, v. 315, pp. 125740, 2022. doi: http://dx.doi.org/10.1016/j.conbuildmat.2021.125740.

[30] SINGH, A., WANG, Y., ZHOU, Y., *et al*., "Utilization of antimony tailings in fiber-reinforced 3D printed concrete: a sustainable approach for construction materials", *Construction & Building Materials*, v. 408, pp. 133689, 2023. doi: http://dx.doi.org/10.1016/j.conbuildmat.2023.133689.

[31] YAO, X., LYU, X., SUN, J., *et al*., "AI-based performance prediction for 3D-printed concrete considering anisotropy and steam curing condition", *Construction & Building Materials*, v. 375, pp. 130898, 2023. doi: http://dx.doi.org/10.1016/j.conbuildmat.2023.130898.

[32] YANG, Y., LIN, B., ZHANG, W., "Experimental and numerical investigation of an arch–beam joint for an arch bridge", *Archives of Civil and Mechanical Engineering*, v. 23, n. 2, pp. 101, 2023. doi: http://dx.doi.org/10.1007/s43452-023-00645-3.

[33] YAO, Y., ZHOU, L., HUANG, H., *et al*., "Cyclic performance of novel composite beam-to-column connections with reduced beam section fuse elements", *Structures*, v. 50, pp. 842–858, 2023. doi: http://dx.doi.org/10.1016/j.istruc.2023.02.054.

[34] ZHANG, W., ZHANG, S., WEI, J., *et al*., "Flexural behavior of SFRC-NC composite beams: An experimental and numerical analytical study", *Structures*, v. 60, pp. 105823, 2024. doi: http://dx.doi.org/10.1016/j.istruc.2023.105823.

[35] HUANG, H., LI, M., ZHANG, W., *et al*., "Seismic behavior of a friction-type artificial plastic hinge for the precast beam–column connection", *Archives of Civil and Mechanical Engineering*, v. 22, n. 4, pp. 201, 2022. doi: http://dx.doi.org/10.1007/s43452-022-00526-1.

[36] LONG, X., MAO, M., SU, T., *et al*., "Machine learning method to predict dynamic compressive response of concrete-like material at high strain rates", *Defence Technology*, v. 23, pp. 100–111, 2023. doi: http://dx.doi.org/10.1016/j.dt.2022.02.003.

[37] ZHANG, C., ABEDINI, M., "Strain rate influences on concrete and steel material behavior, state-of-the-art review", *Archives of Computational Methods in Engineering*, v. 30, n. 7, pp. 4271–4298, 2023. doi: http://dx.doi.org/10.1007/s11831-023-09937-6.

[38] GHASEMI, M., ZHANG, C., KHORSHIDI, H., *et al*., "Seismic upgrading of existing RC frames with displacement-restraint cable bracing", *Engineering Structures*, v. 282, pp. 115764, 2023. doi: http://dx.doi.org/10.1016/j.engstruct.2023.115764.

[39] WEI, J., YING, H., YANG, Y., *et al*., "Seismic performance of concrete-filled steel tubular composite columns with ultra high performance concrete plates", *Engineering Structures*, v. 278, pp. 115500, 2023. doi: http://dx.doi.org/10.1016/j.engstruct.2022.115500.

[40] WANG, X., LI, L., XIANG, Y., *et al*., "The influence of basalt fiber on the mechanical performance of concrete-filled steel tube short columns under axial compression", *Frontiers in Materials*, v. 10, pp. 1332269, 2024. doi: http://dx.doi.org/10.3389/fmats.2023.1332269.

[41] ZHANG, X., ZHOU, G., LIU, X., *et al*., "Experimental and numerical analysis of seismic behaviour for recycled aggregate concrete filled circular steel tube frames", *Computers and Concrete*, v. 31, n. 6, pp. 537–543, 2023. doi: http://dx.doi.org/10.12989/cac.2023.31.6.537.

[42] ZHANG, X., LIU, X., ZHANG, S., *et al*., "Analysis on displacement-based seismic design method of recycled aggregate concrete-filled square steel tube frame structures", *Structural Concrete*, v. 24, n. 3, pp. 3461–3475, 2023. doi: http://dx.doi.org/10.1002/suco.202200720.

[43] LI, H., YANG, Y., WANG, X., *et al*., "Effects of the position and chloride-induced corrosion of strand on bonding behavior between the steel strand and concrete", *Structures*, v. 58, pp. 105500, 2023. doi: http://dx.doi.org/10.1016/j.istruc.2023.105500.

[44] LIU, W., LIANG, J., XU, T., "Tunnelling-induced ground deformation subjected to the behavior of tail grouting materials", *Tunnelling and Underground Space Technology*, v. 140, pp. 105253, 2023. doi: http://dx.doi.org/10.1016/j.tust.2023.105253.

[45] REN, C., YU, J., ZHANG, C., *et al*., "Micro–macro approach of anisotropic damage: a semi-analytical constitutive model of porous cracked rock", *Engineering Fracture Mechanics*, v. 290, pp. 109483, 2023. doi: http://dx.doi.org/10.1016/j.engfracmech.2023.109483.